Organocatalyzed Living Radical Polymerization via in Situ Halogen Exchange of Alkyl Bromides to Alkyl Iodides

Xiao, Longqiang; Sakakibara, Keita; Tsujii, Yoshinobu; Goto, Atsushi

2017

Xiao, L., Sakakibara, K., Tsujii, Y., & Goto, A. (2017). Organocatalyzed Living Radical Polymerization via in Situ Halogen Exchange of Alkyl Bromides to Alkyl Iodides. Macromolecules, 50(5), 1882-1891.

https://hdl.handle.net/10356/81321

https://doi.org/10.1021/acs.macromol.6b02813

Organocatalyzed Living Radical Polymerization via In Situ Halogen Exchange of Alkyl Bromides to Alkyl Iodides

Longqiang Xiao,[1] Keita Sakakibara,[2] Yoshinobu Tsujii,[2] Atsushi Goto[1]**

[1]Division of Chemistry and Biological Chemistry, School of Physical and Mathematical Sciences, Nanyang Technological University, 21 Nanyang Link, 637371 Singapore

[2]Insitute for Chemical Research, Kyoto University, Gokasho, Uji, Kyoto 611-0011, Japan

KEYWORDS: halogen exchange, alkyl bromides, sodium iodide, alkyl iodides, living radical polymerization.

ABSTRACT: Halogen exchange of alkyl bromide (R-Br) with sodium iodide (NaI) was used for the transformation of R-Br to alkyl iodide (R-I) in situ in organocatalyzed living radical polymerization (LRP). R-Br was employed as a starting compound (precursor), and the R-I formed in situ was employed as an initiating dormant species for the polymerization. The efficiency of the transformation significantly depends on the R group of R-Br. By the rational selection of the R group and reaction temperature along with the use of tetrabutylammonium iodide (Bu_4NI) as a catalyst, low-polydispersity (M_w/M_n = 1.1–1.4) polymers were obtained with high conversions (e.g., 70–90%) in reasonably short periods of time (typically 3–10 h) in the polymerizations of methyl methacrylate, butyl acrylate, styrene, acrylonitrile, and functional methacrylates. Well-defined diblock and triblock copolymers and a chain-end functional polymer were also obtained. R-Br is generally much more stable than R-I upon storage. Various R-Br are commercially available. The use of simple, stable, and inexpensive R-Br as precursors of the dormant species is an attractive feature of this system. The high monomer versatility and the accessibility to a wide range of polymer structural designs demonstrated in this work show the capability of this system for use in a range of applications.

INTRODUCTION

Living radical polymerization (LRP) (or reversible deactivation radical polymerization (RDRP)) is a useful technique for tailoring polymer architectures with predictable molecular weights (or molar masses) and narrow molecular weight distributions.[1-15] LRP is based on the reversible activation of a dormant species (Polymer-X) to a propagating radical (Polymer•) (Scheme 1a). We developed organocatalyzed LRP using iodine as a capping agent (X) and organic molecules as catalysts (Scheme 1b).[16-20] Attractive features of this LRP include no use of special capping agents or expensive catalysts. The catalysts include tertiary amines such as triethylamine[17] and organic salts such as tetrabutylammonium iodide ($Bu_4N^+I^-$ (BNI)).[18] These catalysts are relatively non-toxic, easy to handle, and amenable to a wide range of monomers.

Scheme 1. Reversible activation: (a) General scheme of LRP and (b) organocatalyzed LRP.

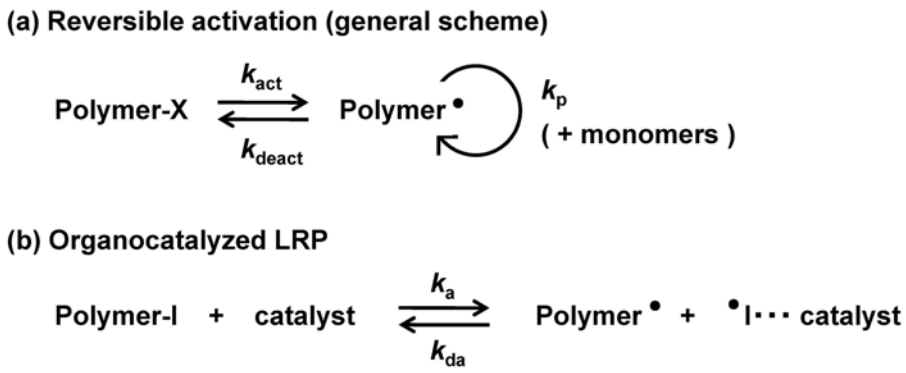

In the previous studies,[16-20] we employed alkyl iodides (R-I) as starting components (dormant species). However, alkyl iodides generally lack long-term stability upon storage, and a limited number of alkyl iodides are commercially available. Alkyl bromides (R-Br) are much more stable than alkyl iodides. A range of alkyl bromides are commercially available and can also be

synthesized. Atom transfer radical polymerization (ATRP) uses alkyl bromides as dormant species and transition metal complexes as catalysts.[3-6] The use of simple, stable, and inexpensive alkyl bromides as the dormant species is an attractive feature of ATRP.

In organic chemistry, the halogen exchange reaction of R-Br with sodium iodide (NaI) is effectively used for the transformation of R-Br to R-I.[21,22] This reaction motivated us to employ R-Br as a starting compound (as a precursor of the dormant species) and NaI as an iodinating agent in organocatalyzed LRP; then, the R-I formed in situ can be used as the dormant species for the polymerization. An important point to consider is that the transformation rate significantly depends on the R group of R-Br. As discussed below, a unimer model of a polymethacrylate bromide, EMA-Br (Figure 1), is not transformed to the corresponding iodide EMA-I in a sufficiently high rate. The rational selection of the R group is a challenge in this study; we eventually found that EPh-Br (Figure 1) and EEMA-Br (Figure 1) are feasible precursors at mild temperatures. EPh-Br and EEMA-Br are structurally simple and commercially available.

Herein, we report the use of R-Br in organocatalyzed LRP via in situ transformation of R-Br to the R-I dormant species in the presence of NaI. This work is the first use of R-Br as starting compounds in organocatalyzed LRP. The use of R-Br overcomes the drawback of the use of isolated R-I, i.e., its general lack of long-term stability upon storage, and thus can significantly widen the scope of organocatalyzed LRP and be highly suitable for practical use. The studied monomers are methyl methacrylate (MMA), butyl acrylate (BA), styrene (St), acrylonitrile (AN), and several functional methacrylates (Figure 1). We studied the syntheses of homopolymers, diblock and triblock copolymers, and a chain-end functional polymer, demonstrating the high

monomer versatility and the accessibility to a wide range of polymer architectural designs. We also conducted a mechanistic study of the transformation reaction in low-mass systems.

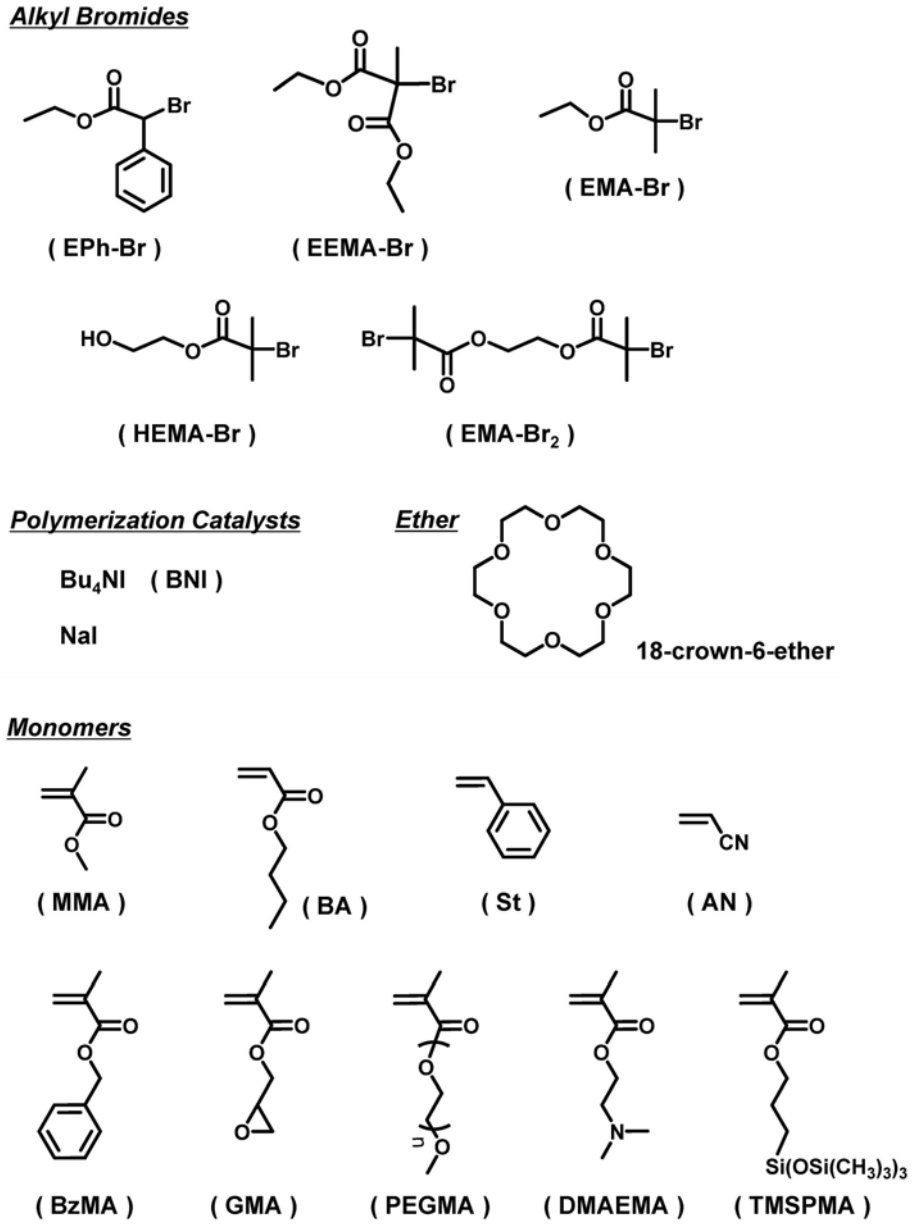

Figure 1. Structures of alkyl bromides, catalysts, crown ether, and monomers used in this work.

RESULTS AND DISCUSSION

Study of Transformation of R-Br to R-I. We studied the transformation of R-Br with NaI to generate R-I in low-mass systems. We used EPh-Br (80 mM (1 eq)) and NaI (90 mM (1.13 eq)) in acetone-d_6. A slight excess of NaI was used to ensure completion of the reaction. The reaction of R-Br and NaI to form R-I and NaBr is reversible. Because a carbon-bromide bond is stronger than a carbon-iodide, the equilibrium between R-Br and R-I can be shifted to R-Br thermodynamically. However, this system is special with respect to the solvent (i.e., solubility of NaI and NaBr). In this system, the generated NaBr is insoluble in acetone, while the reactant NaI is soluble, and hence, the equilibrium is predominantly shifted to the generation of R-I (Scheme 2). This reaction mechanism (to effectively transform R-Br to R-I) is called the Finkelstein reaction.[21,22] Figure 2a shows the ^{1}H NMR spectrum after 10 min at room temperature. EPh-Br was transformed to EPh-I nearly quantitatively (yield = 93%) in a short period of time (10 min) (Figure 2 and Table 1 (entry 1)). Thus, the transformation is very rapid for EPh-Br even at room temperature. Similarly, EEMA-Br was effectively converted to EEMA-I in a high yield (70 %) within 10 min at room temperature (Figure S1 in Supporting Information and Table 1 (entry 2)). Although EEMA-Br (tertiary alkyl bromide) has larger steric hindrance than EPh-Br (secondary alkyl bromide), the transformation still effectively proceeded for the sterically hindered EEMA-Br.

Scheme 2. Halogen Exchange of Bromide with Iodide.

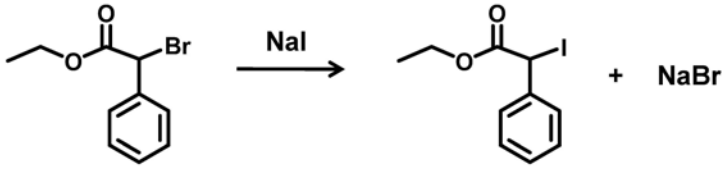

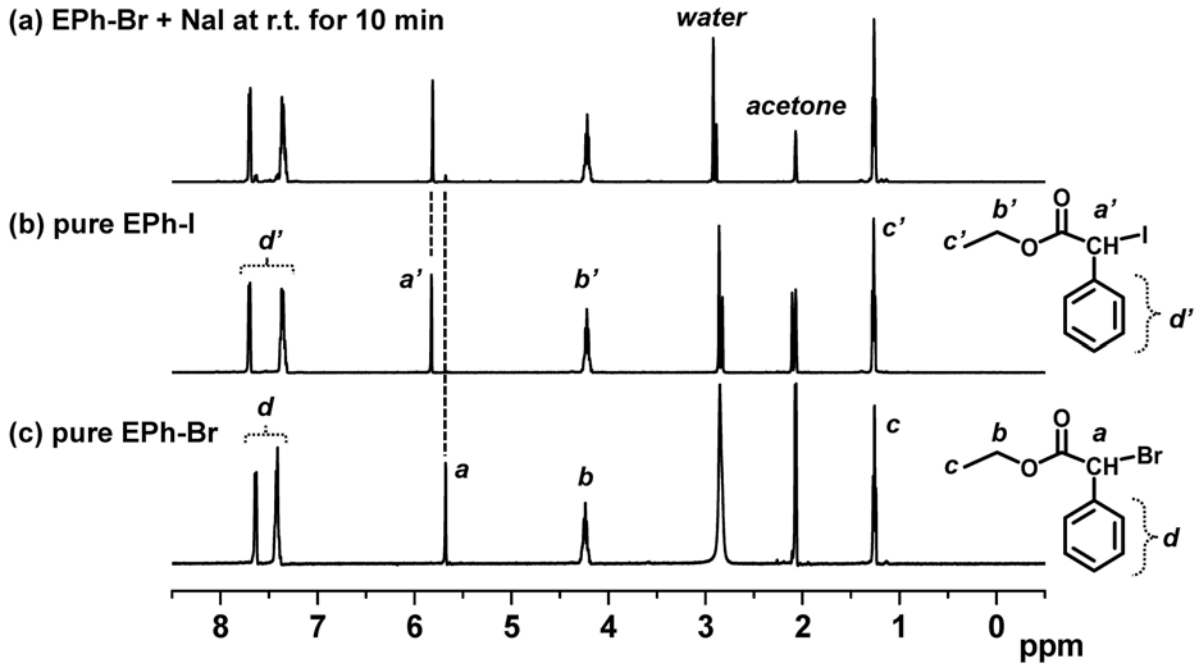

Figure 2. ^{1}H NMR spectra of acetone-d_6 solutions of (a) EPh-Br (80 mM) and NaI (90 mM) at r.t. for 10 min, (b) pure EPh-I, and (c) pure EPh-Br.

Table 1. Halogen Exchange of R-Br (80 mM) with Iodinating Agent (90 mM).

entry	R-Br	Iodinating agent	solvent	T (^{o}C)	t (min)	Observed compounds (%)	
						R-Br	R-I
1	EPh-Br	NaI	acetone-d_6	r.t.	10	7	93
2	EEMA-Br	NaI	acetone-d_6	r.t.	10	30	70
3	EMA-Br	NaI	acetone-d_6	50	240	100	0
4	EPh-Br	NaI	acetone-d_6 / toluene-d_8 = 30/70	r.t.	10	45	55
5	EPh-Br	NaI	acetone-d_6 / toluene-d_8 = 30/70	50	10	18	72
6	EPh-Br	BNI	acetone-d_6 / toluene-d_8 = 30/70	r.t.	10	79	21
7	EPh-Br	BNI	acetone-d_6 / toluene-d_8 = 30/70	50	10	57[a]	18[a]

[a] 57% R-Br, 18% R-I, and 25% side product.

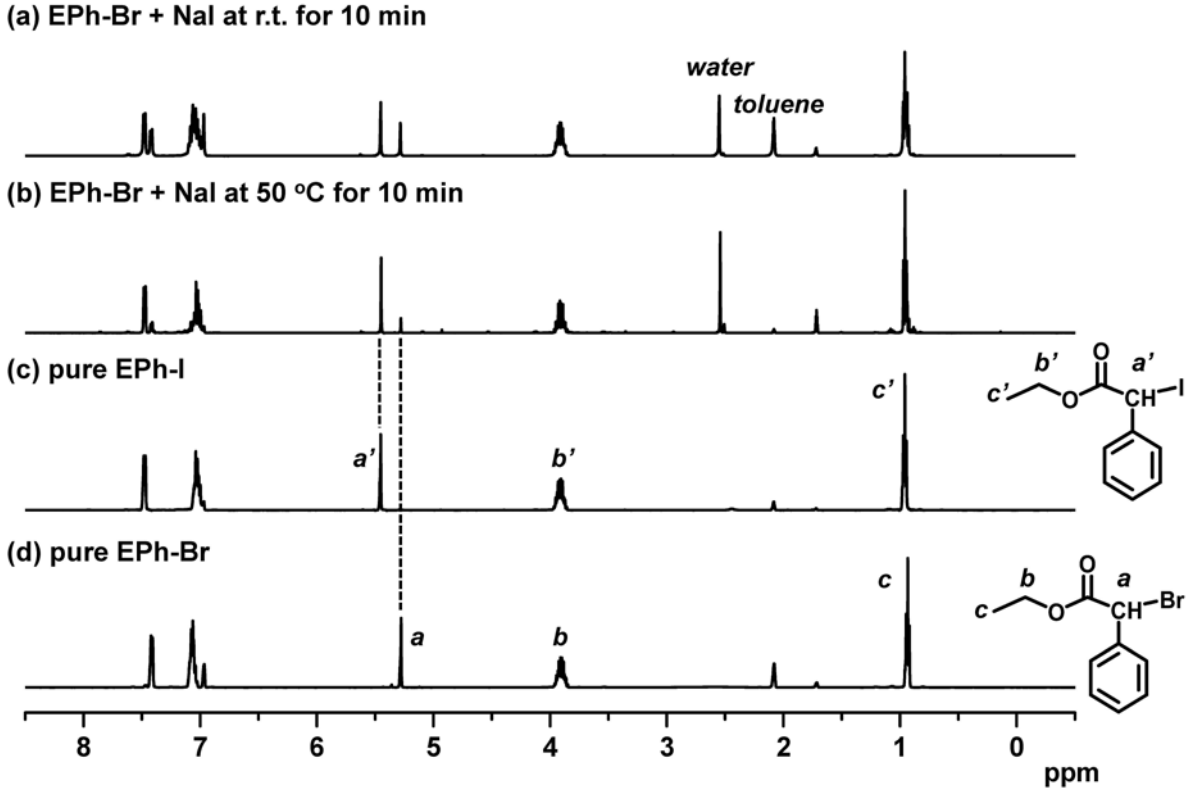

Figure 3. ^{1}H NMR spectra of acetone-d_6/toluene-d_8 (30/70) solutions of EPh-Br (80 mM) and NaI (90 mM) (a) at r.t. for 10 min and (b) at 50 ^{o}C for 10 min, (c) pure EPh-I, and (d) pure EPh-Br.

Unlike EPh-Br and EEMA-Br, the transformation was slow for EMA-Br. Virtually no reaction occurred even at an elevated temperature of 50 °C for 4 h (Figure S2 and Table 1 (entry 3)). The boiling point of acetone is 56 °C, and thus we studied this reaction at 50 °C. EPh-Br and EEMA-Br bear two stabilizing groups (an ester and a phenyl group for EPh-Br and two ester groups for EEMA-Br), while EMA-Br bears only one stabilizing group (an ester group). An inductive effect would also be important. EEMA-Br with two carbonyl groups makes the central carbon more electrophilic and susceptible to this substitution reaction. The selection of the R group of R-Br is important.

The reaction rate depends on the solvent. As a model of MMA medium (dielectric constant ε = 7.9), we used a mixed solvent of 30% acetone-d_6 (ε = 20.7) and 70% toluene-d_8 (ε = 2.4) for the transformation of EPh-Br (Figure 3 and Table 1 (entries 4 and 5)). The reaction was slower in the mixed solvent than in pure acetone-d_6 (yield = 55% and 93%, respectively, after 10 min at room temperature). In the mixed solvent system, an increase of temperature to 50 °C effectively enhanced the reaction; the yield increased to 72% after 10 min. This result clearly suggests that the transformation of EPh-Br to EPh-I is sufficiently fast in the MMA polymerization (MMA medium at 60-70 °C) studied below.

Instead of NaI, we attempted to use BNI as an iodinating agent for EPh-Br (Figure S3 and Table 1 (entries 6 and 7)). The reaction was relatively slow (yield = 21% at room temperature and 18% at 50 °C both for 10 min). An unidentified side product was also generated at 50 °C (25% side product for 10 min). NaI thus afforded finer transformation, although BNI may still be used as a moderately effective iodinating agent.

Polymerizations of MMA. We studied the bulk polymerizations of MMA (8 M, 100 eq) containing R-Br (80 mM, 1 eq) as a precursor of the dormant species, NaI (90 mM, 1.13 eq) as an iodinating agent, and BNI (90 mM, 1.13 eq) as a polymerization catalyst at 60 °C. The molar ratio of MMA to R-Br was 100. Assuming that all of the R-Br is transformed to an initiating dormant species R-I, the degree of polymerization (DP) expected at a 100% monomer conversion is 100. A slight excess of NaI (90 mM) to R-Br (80 mM) was used to ensure complete transformation.

Figure 4 (circles) and Table 2 (entry 1) show the result with EMA-Br as R-Br. No polymerization took place for 12 h. This is attributed to virtually no transformation of EMA-Br to EMA-I. EMA-Br (with one stabilizing group) was thus replaced with EPh-Br (with two

stabilizing groups) (Figure 4 (squares) and Table 2 (entry 3)). Because of the rapid transformation of EPh-Br (as observed above), uniform initiation was attained. The monomer conversion reached 83% in 12 h. The number-average molecular weight (M_n) agreed with the theoretical value ($M_{n,theo}$), and the polydispersity index (PDI) (= M_w/M_n) (or dispersity) was approximately 1.1 from an early stage of polymerization, where M_w is the weight-average molecular weight. We also used EEMA-Br (with two stabilizing groups) (Figure 4 (triangles) and Table 2 (entry 9)). The polymerization was well controlled as in the case of EPh-Br. These results demonstrate the effective use of EPh-Br and EEMA-Br in BNI-catalyzed LRP.

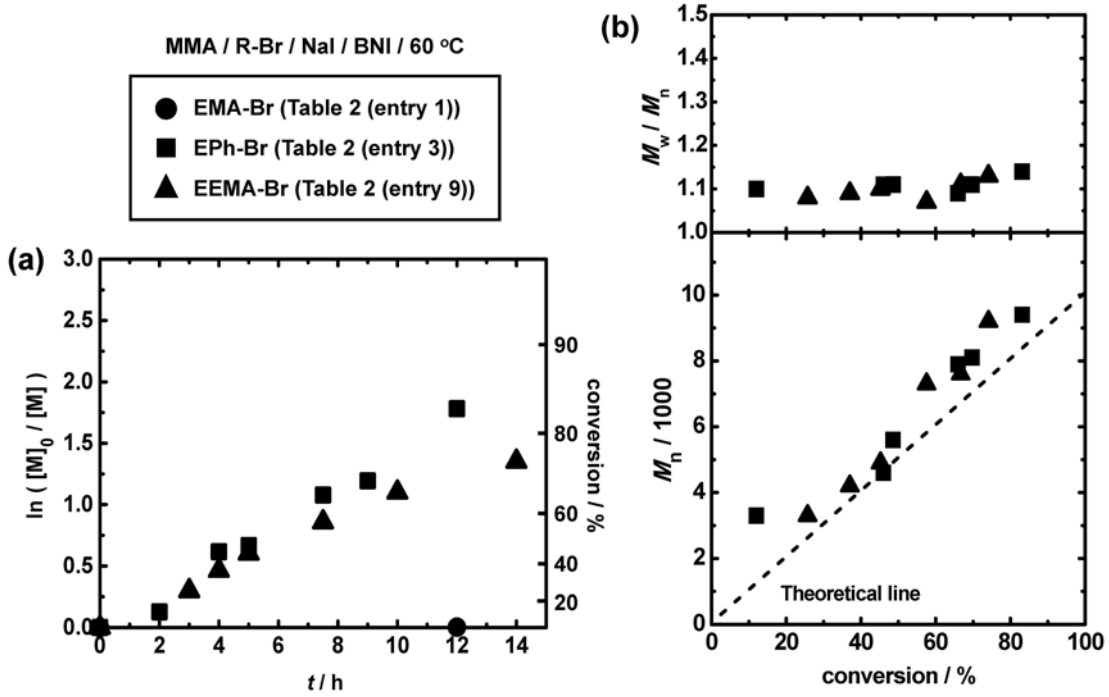

Figure 4. Plots of (a) $\ln([M]_0/[M])$ vs t and (b) M_n and M_w/M_n vs conversion for the MMA/R-Br/NaI/BNI systems (60 °C): $[MMA]_0$ = 8 M; $[R\text{-}Br]_0$ = 80 mM; $[NaI]_0$ = 90 mM; $[BNI]_0$ = 90 mM. The symbols are indicated in the figure.

Table 2. Bulk Polymerizations of MMA.

entry	target DP[a]	R-Br	$[MMA]_0/[R\text{-}Br]_0/[NaI]_0/[BNI]_0/[V65]_0$ (mM)	T (°C)	t (h)	conv (%)	M_n ($M_{n,theo}$[b])	PDI
1	100	EMA-Br	8000/80/90/90/0	60	12	0	–	–
2	100	EMA-Br	8000/80/90/90/0	70	5	26	25000 (2600)	1.51
3	100	EPh-Br	8000/80/90/90/0	60	12	83	9400 (8300)	1.14
4	100	EPh-Br	8000/80/90/90/0	70	3	87	11000 (8700)	1.17
5	100	EPh-Br	8000/80/90/90/10	60	3	84	8400 (8400)	1.18
6	200	EPh-Br	8000/40/45/90/0	70	6	79	17000 (16000)	1.31
7	400	EPh-Br	8000/20/22.5/90/2	70	7	83	30000 (33000)	1.31
8	800	EPh-Br	8000/10/11.25/90/2	70	7	74	50000 (59000)	1.31
9	100	EEMA-Br	8000/80/90/90/0	60	14	74	9200 (7400)	1.13
10	100	EEMA-Br	8000/80/90/90/0	70	4	83	10000 (8300)	1.16
11	100	EEMA-Br	8000/80/90/90/10	60	3	87	9000 (8700)	1.14
12	200	EEMA-Br	8000/40/45/90/0	70	6	74	18000 (15000)	1.24
13	400	EEMA-Br	8000/20/22.5/90/2	70	7	90	37000 (36000)	1.38
14	800	EEMA-Br	8000/10/11.25/90/2	70	7	72	57000 (57000)	1.34
15	100	EPh-Br	8000/80/160/0/0[c]	70	3	82	9200 (8200)	1.20
16	100	EEMA-Br	8000/80/160/0/0[c]	70	3	78	10000 (7800)	1.21
17	100	EPh-Br	8000/80/0/160/0	70	9	58	7400 (5800)	1.31
18	100	EEMA-Br	8000/80/0/160/0	70	9	54	8100 (5400)	1.28

[a]Target degree of polymerization at 100% monomer conversion (calculated by $[MMA]_0/[R\text{-}Br]_0$). [b]Theoretical M_n calculated with $[M]_0$, $[R\text{-}Br]_0$, and monomer conversion. [c]18-crown-6-ether (80 mM) was added.

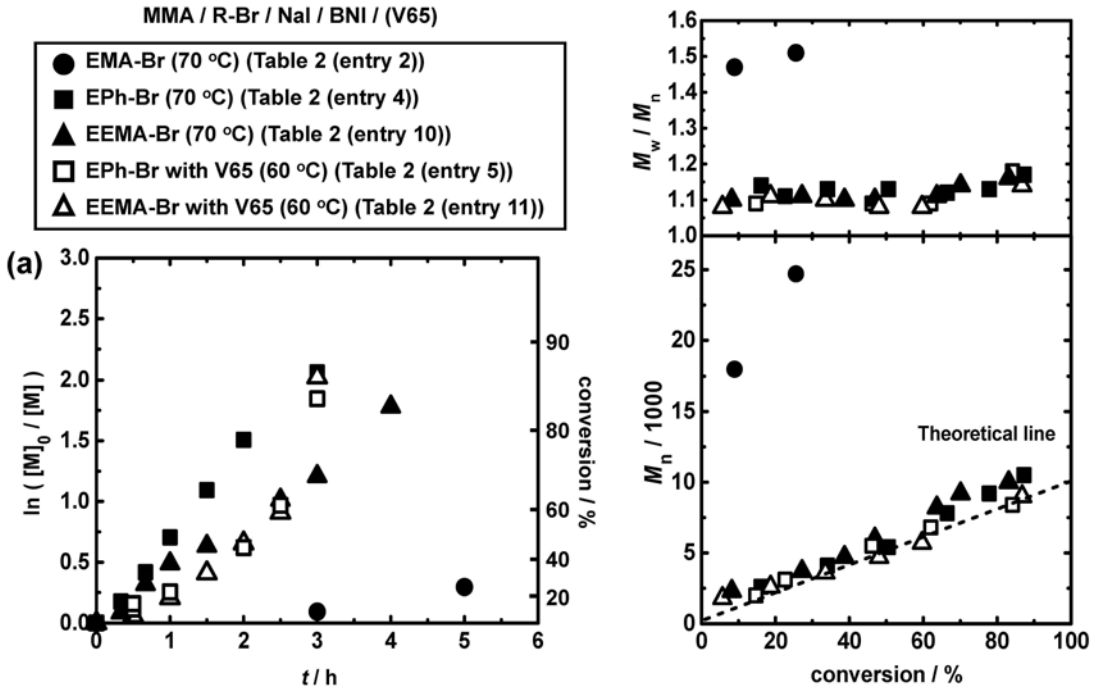

Figure 5. Plots of (a) $\ln([M]_0/[M])$ vs t and (b) M_n and M_w/M_n vs conversion for the MMA/R-Br/NaI/BNI/(V65) systems (60 or 70 ^oC): $[MMA]_0$ = 8 M; $[R\text{-}Br]_0$ = 80 mM; $[NaI]_0$ = 90 mM; $[BNI]_0$ = 90 mM; $[V65]_0$ = 0 or 10 mM. The symbols are indicated in the figure.

Increase of Polymerization Rate. In the above polymerizations with EPh-Br and EEMA-Br, a relatively long time was required to achieve a high monomer conversion (e.g., 83% in 12 h). To increase the polymerization rate (R_p), we elevated the temperature from 60 °C to 70 °C for EPh-Br (Figure 5 (filled squares) and Table 2 (entry 4)) and EEMA-Br (Figure 5 (filled triangles) and Table 2 (entry 10)). The R_p became approximately 4 times larger in both cases; the monomer conversion reached 83-87% in 3-4 h. Another effective way to increase R_p was the addition of a small amount of an azo initiator V65 at 60 °C (Figure 5 (open symbols) and Table 2 (entries 5 and 11)). Azo initiators are often used to decrease the deactivator concentration and hence effectively increase R_p in other LRP systems such as ATRP and nitroxide-mediated

polymerization.[15] Compared with the system without V65 at 60 °C, the addition of V65 (10 mM) increased R_p by a factor of approximately 3-5 at the same temperature (60 °C). The elevated temperature and added small amounts of V65 did not significantly affect M_n or PDI despite the significant increase in R_p. The relatively high R_p (83-87% monomer conversion in 3-4 h) as well as the small PDI (1.1-1.2) achieved even at high conversions is attractive for practical use.

At an elevated temperature of 70 °C, the polymerization proceeded even with using EMA-Br (with one stabilizing group), although the polymerization rate was low (monomer conversion = 26% in 5 h) (Figure 5 (filled circles) and Table 2 (entry 2)). The M_n largely deviated from $M_{n,theo}$, and PDI was large (>1.5). This is attributed to the slow transformation of EMA-Br to EMA-I (as observed above); namely, EMA-Br was only gradually transformed to EMA-I during the polymerization and the initiation did not start uniformly. Nevertheless, it is still noteworthy that the transformation did occur at 70 °C, while virtually no transformation occurred at 60 °C.

Toward Higher Molecular Weights. We targeted higher DPs of 200, 400, and 800 at a 100% monomer conversion (Figure 6 and Table 2 (entries 6-8 and 12-14)). A small amount of V65 was used for the target DPs of 400 and 800 to increase R_p. We obtained low-polydispersity (PDI = 1.1-1.4) polymers with high conversions in reasonable periods of time (monomer conversion = 72-90% in 6-7 h). At high DPs, the viscosity was particularly high, and the Tromsdorf effect was observed at high conversions (open squares in Figure 6).

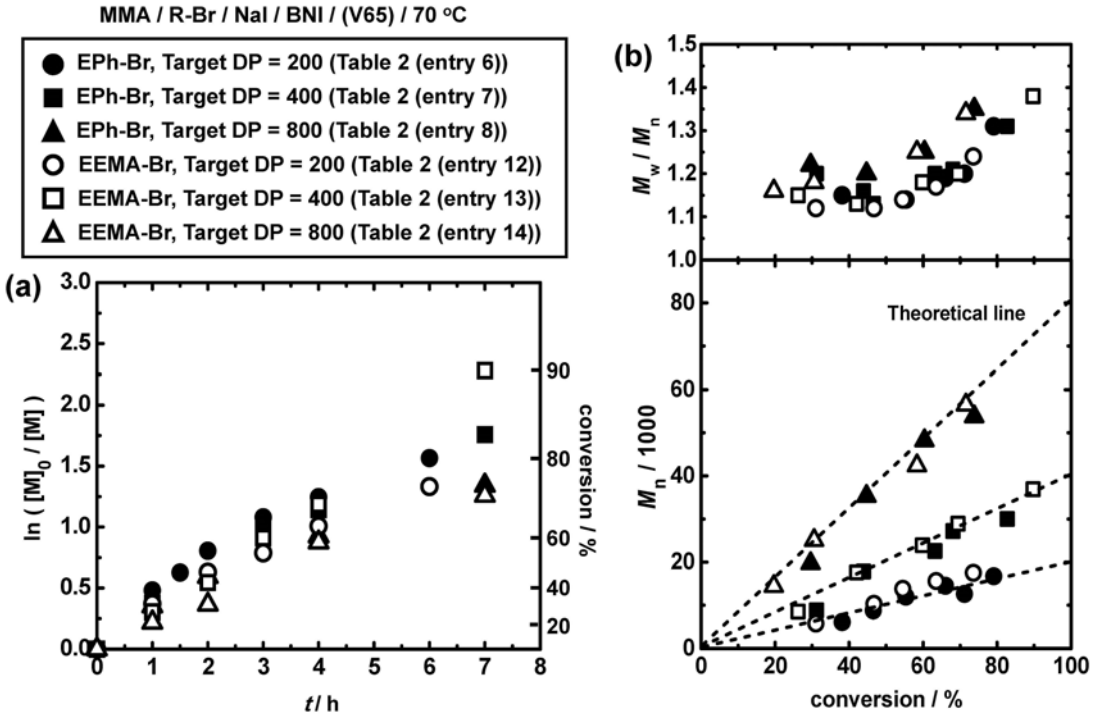

Figure 6. Plots of (a) $\ln([M]_0/[M])$ vs t and (b) M_n and M_w/M_n vs conversion for the MMA/R-Br/NaI/BNI/(V65) systems (70 °C): $[MMA]_0$ = 8 M; $[R\text{-}Br]_0$ = 40, 20, or 10 mM; $[NaI]_0$ = 45, 22.5, or 11.25 mM; $[BNI]_0$ = 90 mM; $[V65]_0$ = 0 or 2 mM. The symbols are indicated in the figure.

Chain-End Fidelity. The chain-ends of a polymer were analyzed. The polymer obtained from EPh-Br at 70 °C after 35 min in Figure 5 (filled squares) (without V65) was reprecipitated in hexane and further purified by preparative GPC to remove any traces of low-mass impurities. The M_n and PDI determined by GPC calibrated with standard poly(methyl methacrylate)s (PMMAs) were 3500 and 1.10, respectively, before the purification, and 3900 and 1.08, respectively, after the purification. Figure 7 shows the 500 MHz ^{1}H NMR spectrum of the polymer after the purification. Acetone-d_6 was used as the NMR solvent to prevent the overlap of the peaks for the chain end groups. The signals of C_6H_5 (7.23-7.37 ppm) and OCH_2CH_3 (3.98-4.16 ppm) at the initiating group were clearly observed, demonstrating the initiation from EPh-I

(in situ generated from EPh-Br). The initiation efficiency was estimated from the relative peak areas of this initiating moiety and the monomer units. We calculated the number of monomer units (= 36) using the M_n determined by GPC and estimated the initiating efficiency to be 90% (with ± 8% experimental error). This result confirms virtually quantitative conversion of EPh-Br for generating polymer.

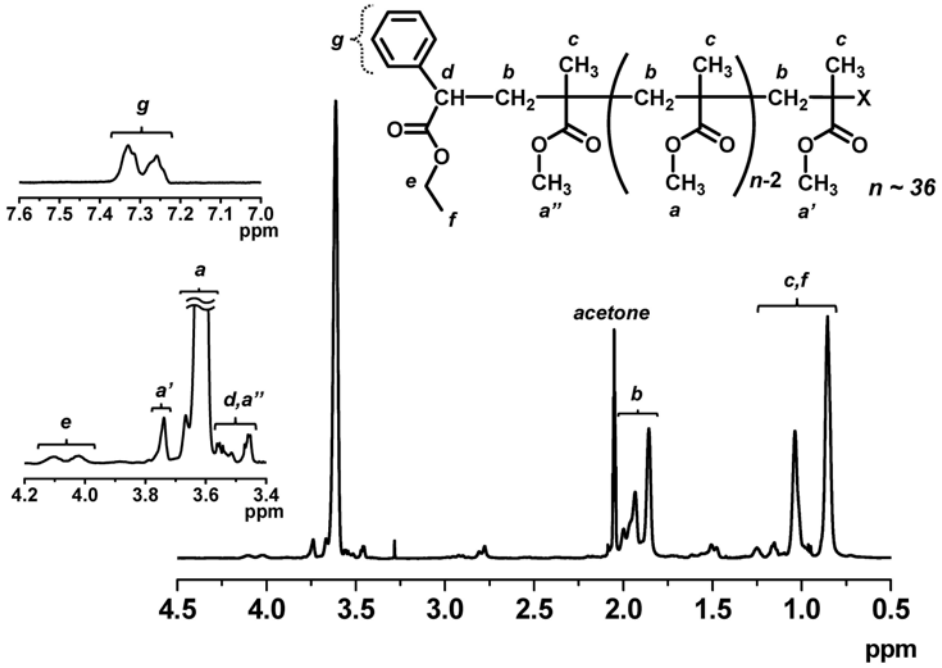

Figure 7. ^{1}H NMR spectrum (acetone-d_6) of PMMA obtained from EPh-Br and purified with preparative GPC (M_n = 3900 and PDI = 1.08 after purification). The polymerization condition is given in Figure 5 (filled square) and Table 2 (entry 4) for 35 min. The chain end group (X) should be bromine or iodine.

In the NMR spectrum, the methyl protons (a, a', and a") at the side chain appeared at 3.43-3.78 ppm. The main peak at 3.57-3.65 ppm and its shoulder peak at 3.65-3.68 ppm were assigned to the monomer units (a) in the middle of the chain (the shoulder peak may be due to a chain-end penultimate unit). The up-field-shifted peaks at 3.43-3.57 would include the α-terminal chain-

end unit (a") adjacent to the initiating group. The down-field-shifted peak at 3.73-3.78 ppm was assigned to the ω-terminal chain-end unit (a') adjacent to a halogen (iodine or bromine). Such a down-field shift for the ω-terminal chain-end unit was reported for PMMA-bromide.[23] From the peak area and the M_n determined by GPC, the fraction of the halogen chain end was calculated to be 100% (92–100% within experimental error). This NMR analysis demonstrates high halogen-chain-end fidelity in this polymerization. To evaluate the iodine/bromine ratio, the polymer was subjected to elemental analysis. The result was 94% of iodine chain-end, 3% of bromine chain-end, and 3% of non-halogen chain-end. Thus, most of the chain-ends were iodine.

To further check the livingness (iodine chain-end fidelity), a chain-extension test was carried out for this polymer (PMMA-X). A mixture of MMA (8 M (400 eq)), PMMA-X (20 mM (1 eq)), and BNI (20 mM (1 eq)) was heated at 70 °C. Figure 8 shows the GPC chromatograms at t = 0 and 4 h. After 4 h, PMMA-X was smoothly extended. Upon the peak resolution, we estimated the inactive polymers (PMMA-Br and terminated chains) remaining in PMMA-X to be at most 10%, confirming the high iodine chain-end fidelity (>90%). (For the peak resolution in Figure 8, we used the distribution of PMMA-X (orange solid line) for determining the remaining polymer (orange dashed line) and subtracted the remaining polymer from the whole polymer (black solid line) for determining the extended polymer (blue dashed line).)

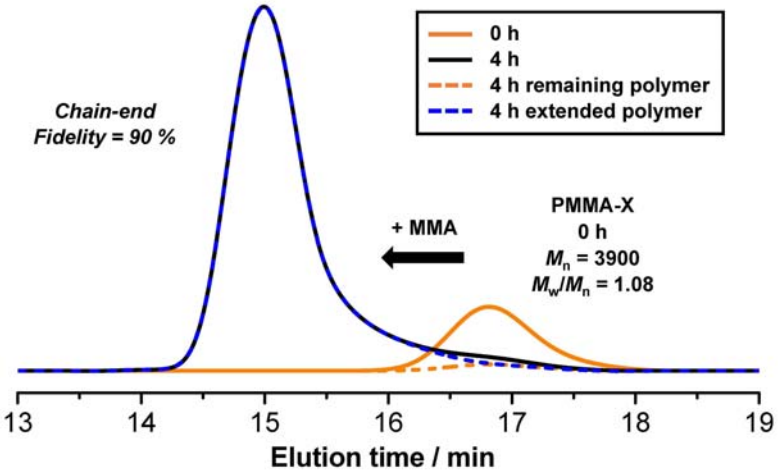

Figure 8. GPC curves for chain-extension of PMMA-X (M_n = 3900 and PDI = 1.08) in the MMA/PMMA-X/BNI system (70 ^oC): $[MMA]_0$ = 8 M; $[PMMA\text{-}X]_0$ = 20 mM; $[BNI]_0$ = 20 mM. The polymerization times and peak resolution are indicated in the figure.

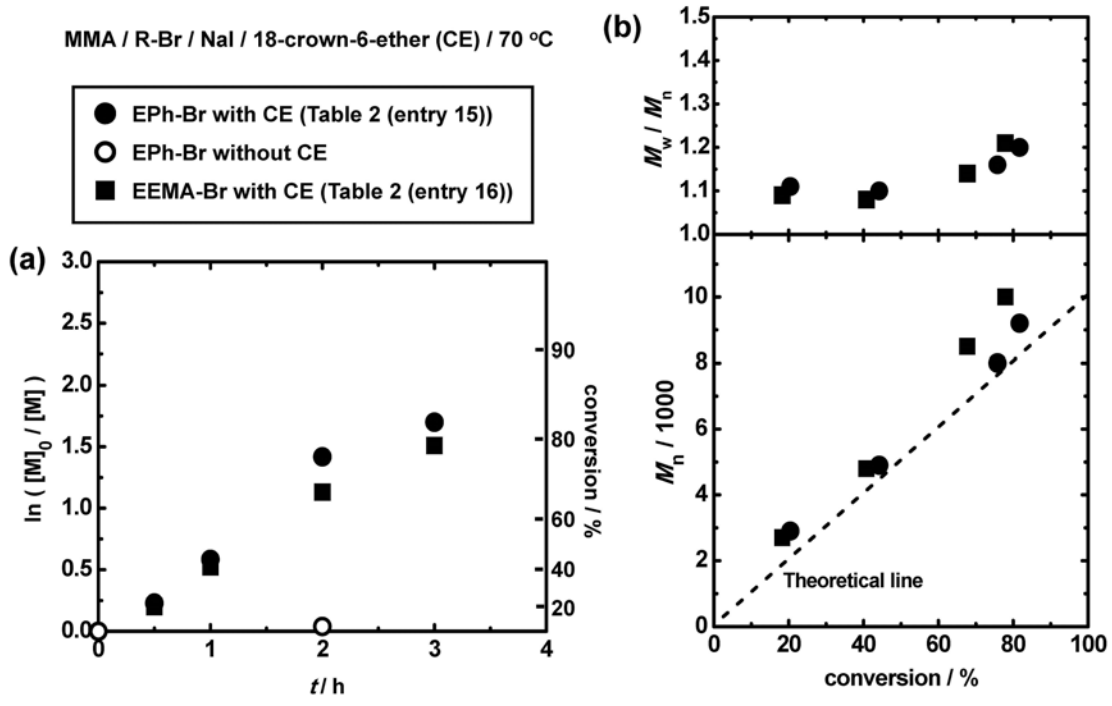

Figure 9. Plots of (a) ln($[M]_0/[M]$) vs t and (b) M_n and M_w/M_n vs conversion for the MMA/R-Br/NaI/18-crown-6-ether (CE) system (70 ^oC): $[MMA]_0$ = 8 M; $[R\text{-}Br]_0$ = 80 mM; $[NaI]_0$ = 160 mM; $[CE]_0$ = 0 or 80 mM; The symbols are indicated in the figure.

Use of NaI as Iodinating Agent and Polymerization Catalyst. In the above-described systems, we added BNI as a polymerization catalyst. We previously reported that NaI can also work as a catalyst.[24] Thus, here, we did not add BNI but used NaI as a polymerization catalyst as well as an iodinating agent. We carried out the polymerizations of MMA (8 M (100 eq)), R-Br (80 mM (1 eq)), NaI (160 mM (2 eq)), and 18-crown-6-ether (80 mM (1 eq)) at 70 °C. One equivalent of NaI was used to transform R-Br to R-I, and the other one equivalent of NaI worked as a polymerization catalyst. One equivalent of 18-crown-6-ether was added for complete dissolution of NaI (as a polymerization catalyst) in MMA. Without the crown-ether, NaI is only partially soluble in MMA. Figure 9 (filled circles and filled squares) and Table 2 (entries 15 and 16) show the results with EPh-Br and EEMA-Br. In both cases, the polymerization was well controlled, as in the BNI-catalyzed system (Figure 5 (filled squares and filled triangles) and Table 2 (entries 4 and 10)), displaying the effective use of NaI as an iodinating agent and a polymerization catalyst. Without 18-crown-6-ether, the polymerization was very slow (Figure 9 (open circle)), because the catalyst NaI was only partially dissolved.

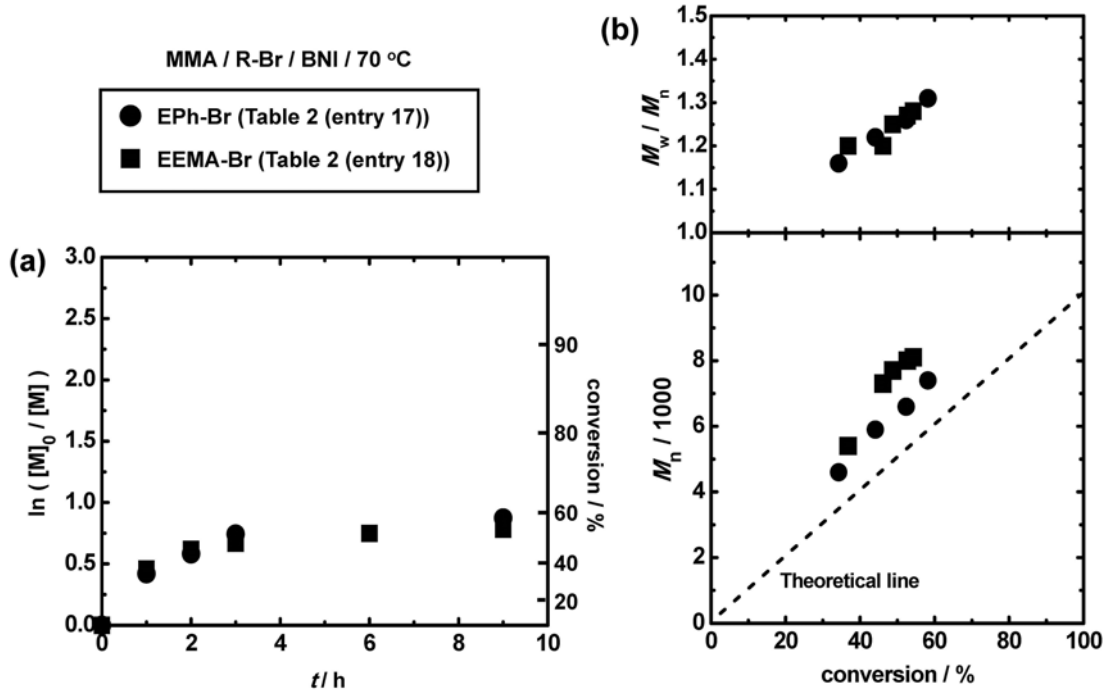

Figure 10. Plots of (a) ln([M]$_0$/[M]) vs t and (b) M_n and M_w/M_n vs conversion for the MMA/R-Br/BNI systems: [MMA]$_0$ = 8 M; [R-Br]$_0$ = 80 mM; [BNI]$_0$ = 160 mM. The symbols are indicated in the figure.

Use of BNI as Iodinating Agent and Polymerization Catalyst. In turn, we used BNI as a polymerization catalyst as well as an iodinating agent (without using NaI). This system is a completely metal-free system. We carried out the polymerizations of MMA (8 M (100 eq)), R-Br (80 mM (1 eq)), and BNI (160 mM (2 eq)) at 70 °C. One equivalent of BNI was used to transform R-Br to R-I, and the other one equivalent of BNI worked as a polymerization catalyst. Figure 10 and Table 2 (entries 17 and 18) show the results with EPh-Br and EEMA-Br. The observed M_n was approximately 30-50% larger than $M_{n,theo}$, meaning that the initiation from R-Br was not quantitative. This result is consistent with the above-mentioned observation that R-Br is converted not only to R-I (dormant species) but also to a side product when BNI is used.

Although the initiation efficiency is not quantitative, the use of BNI as an iodinating agent and a polymerization catalyst may be useful for metal-free applications.

BA, St, AN, and Functional Methacrylates. We studied the polymerizations of BA (8 M (100 eq)) with R-Br (80 mM (1 eq)), NaI (90 mM (1.13 eq)), and BNI (320 mM (4 eq)) at 110 °C. Notably, at this elevated temperature (110 °C), the transformation of R-Br was sufficiently fast even for EMA-Br. (No transformation or only slow transformation of EMA-Br occurred at 60-70 °C as observed above for MMA.) The PDI was approximately 1.4 throughout the polymerization (Figure 11 (circles) and Table 3 (entry 1)). The use of EPh-Br and EEMA-Br led to even lower PDI values (= 1.1-1.3) (Figure 11 (squares and triangles) and Table 3 (entries 2 and 3)). Unexpectedly, the polymerization was faster for EMA-Br than EPh-Br and EEMA-Br. The reason for this behavior is unclear at the moment.

Table 3 shows the polymerizations of St (entry 4), AN (entry 5), and functional methacrylates with benzyl (BzMA), epoxide (GMA), polyethylene glycol (PEGMA), dimethylamino (DMAEMA), and tris(trimethylsilyloxy)silyl (TMSPMA) groups (entries 6-10). In all studied cases, the polymerization was regulated with high conversions (≥71%). These results demonstrate the high monomer versatility of this method. (The molecular weights were obtained with PMMA-calibrated GPC for BA, AN, and functional monomers.)

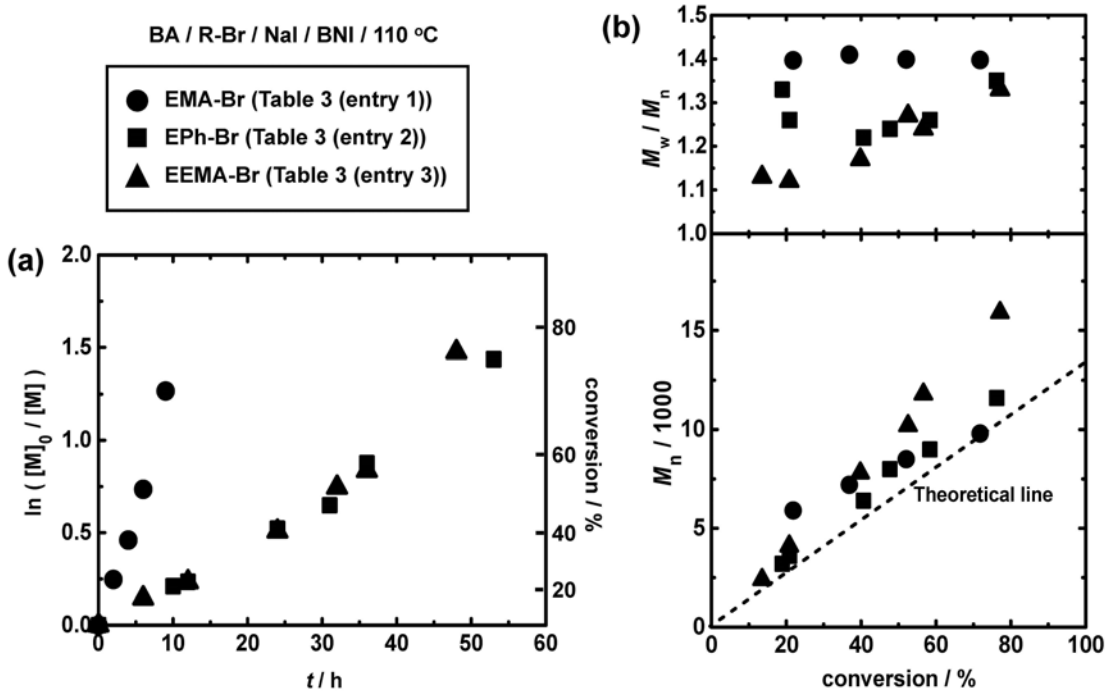

Figure 11. Plots of (a) ln([M]$_0$/[M]) vs t and (b) M_n and M_w/M_n vs conversion for the BA/R-Br/NaI/BNI systems (110 ^oC): [BA]$_0$ = 8 M; [R-Br]$_0$ = 80 mM; [NaI]$_0$ = 90 mM; [BNI]$_0$ = 320 mM. The symbols are indicated in the figure.

Table 3. Bulk polymerizations of Several Monomers.

entry	monomer	target DP[a]	R-Br	azo	[M]$_0$/[R-Br]$_0$/[NaI]$_0$/ [BNI]$_0$/[azo]$_0$ (mM)[b]	T (^{o}C)	t (h)	conv (%)	M_n[c] ($M_{n,theo}$[d])	PDI[c]
1	BA	100	EMA-Br	-	8000/80/90/320/0	110	9	72	9800 (9200)	1.40
2	BA	100	EPh-Br	-	8000/80/90/320/0	110	53	76	16000 (9700)	1.33
3	BA	100	EEMA-Br	-	8000/80/90/320/0	110	48	77	12000 (9800)	1.35
4	St	50	EPh-Br	AIBN	8000/160/180/40/60	80	7	96	4000 (5000)	1.35
5	AN	100	EPh-Br	AIBN	8000/80/90/160/0.5[e]	75	24	74	9100 (3900)	1.30
6	BzMA	100	EPh-Br	V65	8000/80/90/90/10	70	4	71	12000 (12000)	1.23
7	GMA	100	EPh-Br	V65	8000/80/90/90/0	70	2	89	15000 (13000)	1.40
8	PEGMA	100	EPh-Br	AIBN	8000/80/90/90/80	50	4	71	16000 (21000)	1.43
9	DMAEMA	100	EPh-Br	V65	8000/80/90/90/10	50	9	91	19000 (16000)	1.35
10	TMSPMA	50	EPh-Br	-	8000/160/180/180/0	100	10	89	20000 (19000)	1.44

[a]Target degree of polymerization at 100% monomer conversion (calculated by [M]$_0$/[R-Br]$_0$). [b]M = monomer. [c]PMMA-calibrated GPC values for entries 1-3 and 5-10, and polystyrene-calibrated GPC values for entry 4. [d]Theoretical M_n calibrated with [M]$_0$, [R-Br]$_0$, and monomer conversion. [e]Ethylene carbonate (EC) = 50 wt%.

Chain-end Functional Polymer. A chain-end functional polymer was prepared by using a functional alkyl bromide, i.e., HEMA-Br with a hydroxyl group (Figure 1), in the polymerization of BA (Table 4 (entry 1) and Figure 12). An azo initiator (V65) was not used in this case to obtain a pure chain-end functional polymer. Figure 12 shows the ^{1}H NMR spectrum of the polymer synthesized with a monomer conversion of 42% and subsequently purified with a preparative GPC (M_n = 3500 and PDI = 1.20 after purification). The signal of CH_2OH (3.8 ppm) in the initiating moiety was clearly observed, demonstrating the introduction of the hydroxyl group at the chain end. The chain-end functionality can be estimated from the relative peak areas of this initiating moiety and the monomer units. The estimated chain-end functionality was 100-120% (with ± 20% experimental error). Thus, we obtained a polymer with virtually quantitative chain-end functionality.

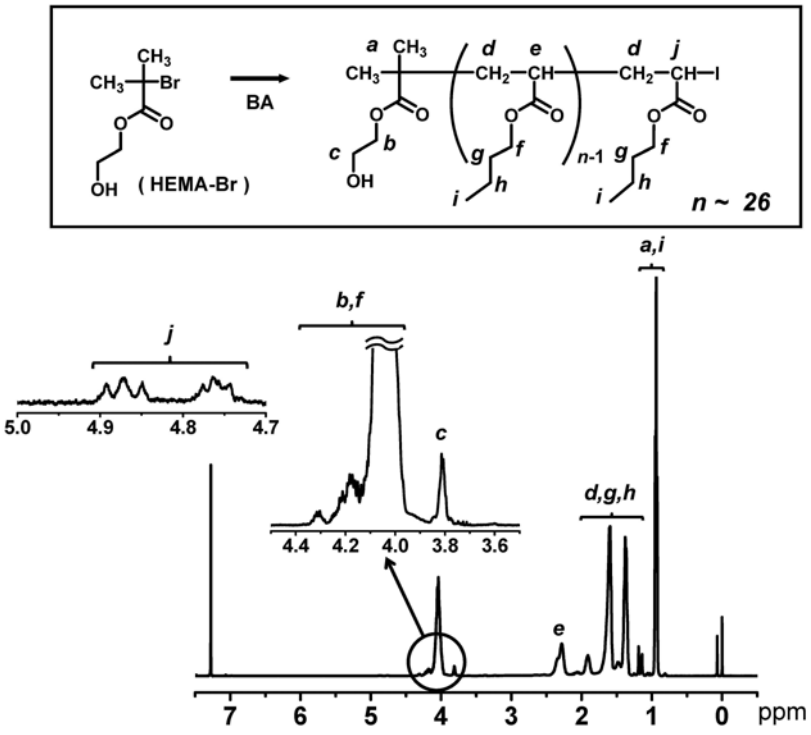

Figure 12. ^{1}H NMR spectrum ($CDCl_3$) of PBA-I obtained from HEMA-Br and purified with preparative GPC (M_n = 3500 and PDI = 1.20 after purification). The polymerization condition is given in Table 4 (entry 1).

Table 4. Bulk Polymerizations of BA with Functional R-Br and R-Br$_2$.

entry	target DP[a]	R-Br	$[M]_0/[R\text{-}Br]_0/[NaI]_0/[BNI]_0$ (mM)[b]	T (°C)	t (h)	conv (%)	M_n[c] ($M_{n,theo}$[d])	PDI[c]
1	50	HEMA-Br	8000/160/180/320	110	12	42	3400 (2700)	1.20
				after purification			3500	1.20
2	200	EMA-Br$_2$	8000/40/90/320	110	30	74	17000 (19000)	1.36
				after purification			18000	1.28

[a]Target degree of polymerization at 100% monomer conversion (calculated by $[M]_0/[R\text{-}Br]_0$). [b]M = monomer. [c]PMMA-calibrated GPC values. [d]Theoretical M_n calibrated with $[M]_0$, $[R\text{-}Br]_0$, and monomer conversion.

Block Polymerizations. Exploiting the living character, we performed block polymerizations. Starting from the purified low-polydispersity PMMA-iodide (PMMA–I) macroinitiator (M_n = 3900 and PDI = 1.08) presented in Figure 7, the polymerizations of GMA and HEMA yielded well-defined block copolymers (Figures 13a and 13b and Table 5 (entries 1 and 2)). Figures 13a and 13b show the full molecular weight distributions (GPC chromatograms). A large fraction of the macroinitiator chains were extended to block copolymers, which confirms high block-efficiency due to the high chain-end fidelity, as demonstrated above (Figure 8).

In addition to the mono-alkyl bromide (R-Br) used above, we employed an alkyl di-bromide EMA-Br$_2$ (Figure 1) to prepare an A-B-A triblock copolymer. BA was used as the first block monomer (B segment monomer) to afford a polymer with M_n = 18000 and PDI = 1.28 after purification (Table 4 (entry 2)). The subsequent polymerization of MMA (A segment monomer) yielded a low-polydispersity MMA-BA-MMA triblock copolymer with M_n = 29000 and PDI = 1.32. These results demonstrate the accessibility of this halogen exchange system to a wide range of polymer architectural designs (di-block, tri-block, and chain-end functional polymers).

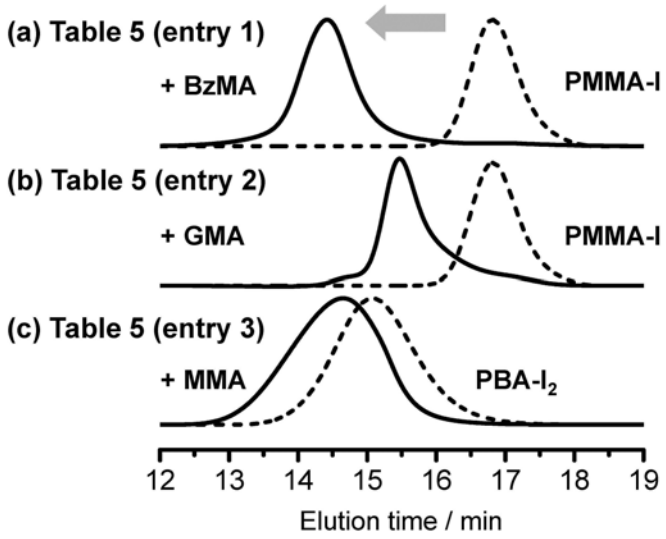

Figure 13. GPC chromatograms before (dashed lines) and after (solid lines) the block polymerizations in Tables 5.

Table 5. Block Polymerizations.

entry	monomer	target DP[a]	R-I[b]	azo	$[M]_0/[R\text{-}I]_0/[BNI]_0/[azo]_0$ (mM)[c]	T (°C)	t (h)	conv (%)	M_n[d] ($M_{n,theo}$[e])	PDI[d]
1	BzMA	200	PMMA-I	V65	8000/40/40/20	60	4	76	22000 (31000)	1.16
2	GMA	100	PMMA-I	-	8000/80/80/0	70	1.5	55	11000 (12000)	1.24
3	MMA	200	PBA-I_2	-	8000/40/80/0[f]	110	16	71	29000 (32000)	1.32

[a]Target degree of polymerization at 100% monomer conversion (calculated by $[M]_0/[R\text{-}I]_0$). [b]R-I = PMMA-I (M_n = 3900 and M_w/M_n = 1.08) prepared after 35 min in Figure 5 (filled squares) and Table 2 (entry 4) and PBA-I_2 (M_n = 18000 and M_w/M_n = 1.28) prepared in Table 4 (entry 2). [c]M = monomer. [d]PMMA-calibrated GPC values. [e]Theoretical M_n calibrated with $[M]_0$, $[R\text{-}I]_0$, and monomer conversion. [f]40 wt% of diglyme was added (60 wt% of a mixture of MMA and PBA-I_2).

CONCLUSIONS

Effective halogen exchange of R-Br with NaI to generate R-I and NaBr was experimentally demonstrated. Based on this proof, R-Br was employed as a starting precursor, and the R-I formed in situ was employed as an initiating dormant species in the BNI-catalyzed

polymerization. The rational selection of the R group and reaction temperature is important. The amenable monomers encompassed MMA, BA, St, AN, and functional methacrylates. Well-defined homopolymers, a chain-end functional polymer, and diblock and triblock copolymers were synthesized. The high stability on storage and wide commercial availability of R-Br and the accessibility to a wide range of polymer designs are highly attractive features of this polymerization.

ASSOCIATED CONTENT

Supporting Information

Experimental Section and halogen exchange experiments. This material is available free of charge via the Internet at http://pubs.acs.org.

AUTHOR INFORMATION

Corresponding Author

*E-mails: agoto@ntu.edu.sg, tsujii@scl.kyoto-u.ac.jp

Notes

The authors declare no competing financial interest.

ACKNOWLEDGMENTS

This work was partly supported by a program of Accelerated Innovation Research Initiative Turning Top Science and Ideas into High-Impact Values (ACCEL) of the Japan Science and Technology Agency (JST) and Start-Up-Grant of Nanyang Technological University.

REFERENCES

(1) Matyjaszewski, K.; Möller, M. *Polymer Science: A Comprehensive Reference*; Elsevier: Amsterdam, 2012.

(2) Tsarevsky, N. V.; Sumerlin, B. S. *Fundamentals of Controlled/Living Radical Polymerization*; Royal Society of Chemistry: UK, 2013.

(3) Matyjaszewski, K.; Tsarevsky, N. V. Macromolecular Engineering by Atom Transfer Radical Polymerization. *J. Am. Chem. Soc.* **2014**, *136*, 6513-6533.

(4) Ouchi, M.; Terashima, T.; Sawamoto, M. Transition Metal-Catalyzed Living Radical Polymerization: Toward Perfection in Catalysis and Precision Polymer Synthesis. *Chem. Rev.* **2009**, *109*, 4963-5050.

(5) Zhang, N.; Samanta, S. R.; Rosen, B. M.; Percec, V. Single Electron Transfer in Radical Ion and Radical-Mediated Organic, Materials and Polymer Synthesis. *Chem. Rev.* **2014**, *114*, 5848-5958.

(6) Boyer, C.; Corrigan, N. A.; Jung, K.; Nguyen, D.; Nguyen, T.-K.; Adnan, N. N. M.; Oliver, S.; Shanmugam, S.; Yeow, J. Copper-Mediated Living Radical Polymerization (Atom Transfer Radical Polymerization and Copper(0) Mediated Polymerization): From Fundamentals to Bioapplications. *Chem. Rev.* **2016**, *116*, 1803-1949.

(7) Nicolas, J.; Guillaneuf, Y.; Lefay, C.; Bertin, D.; Gigmes, D.; Charleux, B. Nitroxide-Mediated Polymerization. *Prog. Polym. Sci.* **2013**, *38*, 63–235.

(8) Keddie, D. J.; Moad, G.; Rizzardo, E.; Thang, S. H. RAFT Agent Design and Synthesis. *Macromolecules* **2012**, *45*, 5321-5342.

(9) David, G.; Boyer, C.; Tonnar, J.; Ameduri, B.; Lacroix-Desmazes, P.; Boutevin, B. Use of Iodocompounds in Radical Polymerization. *Chem. Rev.* **2006**, *106*, 3936-3962.

(10) Yamago, S. Precision Polymer Synthesis by Degenerative Transfer Controlled/Living Radical Polymerization Using Organotellurium, Organostibine, and Organobismuthine Chain-Transfer Agents. *Chem. Rev.* **2009**, *109*, 5051-5068.

(11) Satoh, K.; Kamigaito, M. Stereospecific Living Radical Polymerization: Dual Control of Chain Length and Tacticity for Precision Polymer Synthesis. *Chem. Rev.* **2009**, *109*, 5120-5156.

(12) Zetterlund, P. B.; Thickett, S. C.; Perrier, S.; Bourgeat-Lami, E.; Lansalot, M. Controlled/Living Radical Polymerization in Dispersed Systems: An Update. *Chem. Rev.* **2015**, *115*, 9745-9800.

(13) Chen, M.; Zhong, M.; Johnson, J. A. Light-Controlled Radical Polymerization: Mechanisms, Methods, and Applications. *Chem. Rev.* **2016**, *116*, 10167-10211.

(14) Mastan, E., Li X.; Zhu S. Modeling and Theoretical Development in Controlled Radical Polymerization. *Prog. Polym. Sci.* **2015**, *45*, 71-101.

(15) Goto, A.; Fukuda, T. Kinetics of Living Radical Polymerization. *Prog. Polym. Sci.* **2004**, *29*, 329-385.

(16) Goto, A.; Zushi, H.; Hirai, N.; Wakada, T.; Tsujii, Y.; Fukuda, T. Living Radical Polymerizations with Germanium, Tin, and Phosphorus Catalysts - Reversible Chain Transfer Catalyzed Polymerizations (RTCPs). *J. Am. Chem. Soc.* **2007**, *129*, 13347-13354.

(17) Goto, A.; Suzuki, T.; Ohfuji, H.; Tanishima, M.; Fukuda, T.; Tsujii, Y.; Kaji, H. Reversible Complexation Mediated Living Radical Polymerization (RCMP) Using Organic Catalysts. *Macromolecules* **2011**, *44*, 8709-8715.

(18) Goto, A.; Ohtsuki, A.; Ohfuji, H.; Tanishima, M.; Kaji, H. Reversible Generation of a Carbon-Centered Radical from Alkyl Iodide Using Organic Salts and Their Application as Organic Catalysts in Living Radical Polymerization. *J. Am. Chem. Soc.* **2013**, *135*, 11131-11139.

(19) Ohtsuki, A.; Lei, L.; Tanishima, M.; Goto, A.; Kaji, H. Photocontrolled Organocatalyzed Living Radical Polymerization Feasible over a Wide Range of Wavelengths. *J. Am. Chem. Soc.* **2015**, *137*, 5610-5617.

(20) Chen, C.; Xiao, L.; Goto, A. Comprehensive Study on Chain-End Transformation of Polymer-Iodides with Amines for Synthesizing Various Chain-End Functionalized Polymers. *Macromolecules* **2016**, *49*, 9425-9440.

(21) Finkelstein, H. Darstellung organischer Jodide aus den entsprechenden Bromiden und Ohloriden. *Ber.* **1910**, *43*, 1528−1532.

(22) Pace, R. D.; Regmi Y. The Finkelstein Reaction: Quantitative Reaction Kinetics of an S_N2 Reaction Using Nonaqueous Conductivity. *J. Chem. Edu.* **2006**, *9*, 1344-1348.

(23) Ando, T.; Kamingaito, M.; Sawamoto, M. Iron(II) Chloride Complex for Living Radical Polymerization of Methyl Methacrylate. *Macromolecules* **1997**, *30*, 4507-4510.

(24) Sarker, J.; Xiao, L.; Goto, A. Living Radical Polymerization with Alkali and Alkaline Earth Metal Iodides as Catalysts. *Macromolecules* **2016**, *49*, 5033-5042.

For Table of Contents Use Only (color graphic)